Journal of Non-Crystalline Solids 247 (1999) 79–86

Anisotropic residual stresses in partially crystallized Li_2O–$2SiO_2$ glass-ceramics

Valmor R. Mastelaro [1], Edgar D. Zanotto *

Vitreous Materials Laboratory (LaMaV), Department of Materials Engineering (DEMa), Federal University of São Carlos (UFSCar), CEP 13565-905, São Carlos, SP, Brazil

Abstract

Levels of residual stresses in partially crystallized Li_2O–$2SiO_2$ glass-ceramics were calculated for several crystallographic planes. The stresses were also determined by an X-ray diffraction method (XRD) using synchrotron radiation. The linear thermal expansion coefficient (α_{hkl}) of a fully crystallized, stress-free, powdered sample, was measured in situ using a hot-stage XRD technique. The thermal expansion coefficient depends on the crystallographic (*hkl*) direction. For some direction, the thermal expansion coefficient of the crystalline phase is greater than that of the glass matrix, while for other direction the inverse is observed. The average thermal expansion coefficient calculated from the unit cell expansion with temperature $\alpha_{uc} = (10.1 \pm 0.5) \times 10^{-6}°C^{-1}$ was close to that obtained by a dilatometric method for a polycrystalline sample $\langle\alpha_c\rangle = (10.8 \pm 0.5) \times 10^{-6}°C^{-1}$. The theoretical residual stresses were calculated by the Selsing model using experimental data for the elastic constants combined with the thermal expansion coefficient for each crystallographic plane. Experimental determinations of residual stresses were made using an XRD technique for six different sets of (*hkl*) planes in two partially crystallized specimens. The type of experimental residual stresses (tensile or compressive) for each crystallographic plane was in agreement with the predicted type. Regarding the stress magnitude, the *experimental* results vary from −58/−117 MPa (compressive) to 60/149 MPa (tensile), whereas the *calculated* magnitudes vary from −192 MPa (compressive) to 16/102 MPa (tensile). These magnitudes were confirmed by micro-Raman spectroscopy. The differences between the theoretical and experimental stress magnitudes are within the limits of experimental errors. Therefore, the Selsing model can give a reasonable estimate of residual stresses for real (anisotropic) materials. © 1999 Elsevier Science B.V. All rights reserved.

1. Introduction

Glass-ceramics are polycrystalline materials produced by controlled crystallization of glass having one or more crystal phases embedded in a glassy matrix. The ability to produce complex shapes, coupled to their lack of porosity and microstructure control make glass-ceramics unique for both domestic and advanced applications, such as microwave and opto-electronic devices [1], surgical implants [2] and large telescope mirrors [3]. Their mechanical performance is a major issue in such applications.

The mechanical properties of these materials are dependent on microstructural parameters and also on the level and type (tensile vs. compressive) of residual stresses around the crystals. These stresses increase on cooling specimens from the

* Corresponding author. Tel.: +55-162 748 249; fax: +55-162 727 404; e-mail: dedz@power.ufscar.br

[1] Present address: Institute of Physics of São Carlos, University of São Paulo, Brazil.

0022-3093/99/$ – see front matter © 1999 Elsevier Science B.V. All rights reserved.
PII: S0022-3093(99)00038-1

vicinity of the glass transition temperature, T_g, to room temperature due to the thermal and elastic mismatch between the constituent phases. While the effects of microstructure on mechanical properties are well established, much less is known on the effects of residual stresses. Recently we reported an experimental test of two models often used describe the residual stresses in duplex materials, using a partially crystallized soda–lime–silica glass [4]. The experimental stresses were in good agreement with those calculated using the Selsing model [5]. To generalize the findings of [4], we extend that study here to another silicate system: partially crystallized Li_2O–$2SiO_2$ glass-ceramics.

2. Theory of residual stresses

The deduction of and popularization of the effects of residual thermal stresses in composites containing particulate inclusions was attributed to Selsing [5]. For the particular case of a spherical inclusion of radius, R, embedded in an infinite matrix, subjected to a temperature variation, ΔT, the analytical expression for the stresses in the matrix and in the inclusion can be easily deduced. The stresses in the matrix, for an *isotropic*, elastic material are given by the following equations:

$$\sigma_r = P \cdot (R/x)^3, \tag{1}$$

$$\sigma_\theta = -P/2 \cdot (R/x)^3, \tag{2}$$

where σ_r is the radial stress, σ_θ the tangential stress, P the hydrostatic pressure on the particle, R the particle radius and x the distance from the center of the inclusion. Thus, these stresses are maximum at the crystal/glass interface ($x = R$) and drop to only 3.7% of the maximum for $x = 3R$.

The hydrostatic thermal stress, P, can be obtained using the following equation [5]:

$$P = \Delta\alpha \cdot \Delta T / K_e, \tag{3}$$

where $K_e = [(1 + v_m)/2E_m + (1 - 2v_p)/E_p]$, E and v being respectively the elastic modulus and the Poisson ratio, and the subscripts, m and p, refer to the matrix and particle, respectively. $\Delta\alpha = \alpha_p - \alpha_m$ is the thermal expansion mismatch and ΔT the difference between the temperature at which the glass ceases to flow on cooling ($\approx T_g$) and the ambient temperature.

For an *isotropic* system containing several particles in a matrix, Eq. (3) should still hold if the stress fields around each particle do not overlap. This situation is expected to be valid if the volume percentage of the second phase does not exceed approximately 15% [4]. However, as real materials are seldom isotropic, we will test the validity of Eq. (3) to estimate residual stresses in anisotropic materials, using a $Li_2Si_2O_5$ glass-ceramic.

3. Literature review

Recently we carried out a literature review about residual stresses in glass-ceramics [4] and observed that a controversy remains on this subject. For instance, in the works of Fulrath [6] and Zevin et al. [7], the experimental residual stresses were dependent on the particle size, however, according to Davidge and Green [8] they should not be. In addition, in the papers published by Borom et al. [9] and Miyata et al. [10] the experimental internal stresses were smaller than the calculated stresses (using Eq. (3)). Although there are several new publications on residual stresses in other materials, a literature search, using the 'Web of Science' database of the Institute of Scientific Information (ISI), which includes all periodicals indexed by the ISI, did not reveal any recent paper about residual stresses in glass-ceramics.

4. Materials and methods

4.1. Sample preparation

The Li_2O–$2SiO_2$ system was chosen because it presents favorable conditions for the residual stresses study, principally concerning the facility of microstructure control, and also due to the fact that this system has been extensively studied by our research group [11].

A glass of Li_2O–$2SiO_2$ composition was melted at 1350°C in a Pt crucible in air. The liquid was then cast between two cold steel plates, with an

estimated cooling rate of 400°C/min. To obtain partially crystallized glasses (glass-ceramics), some specimens, $10 \times 25 \times 3$ mm, were submitted to isothermal treatments at 460°C ($T_g \sim 450$°C) for two different periods, 86 and 100 h. The heat treatments were carried out in an electric furnace with a temperature control within ±1°C. A fully crystallized polycrystalline sample, used for thermal expansion measurements, and a powdered sample, used as a stress free standard, were obtained by nucleating one specimen at 450°C for 24 h and then heating it at 600°C for 10 min to allow crystal growth. Only the stable $Li_2Si_2O_5$ crystalline phase was detected after these heat treatments.

4.2. Microstructure and physical properties

After polishing and etching glass-ceramic plates by a diluted solution of HF/HCl (0.08%/0.04%) for 30 s, they were observed by reflected light microscopy (RLM) coupled to an image analyzer system. The experimental crystallized fraction of the samples were about 8% for the sample heat-treated for 86 h, and 10% for the sample heat-treated for 100 h.

The crystal morphology was observed by RLM. Fig. 1 shows an RLM micrograph of the specimen heat-treated for 100 h at 460°C. For this treatment, the $Li_2Si_2O_5$ crystals have an ellipsoidal geometry and a maximum size of approximately 12 μm. We did not observe the formation of crystal branches, reported for specimens heat-treated in different conditions [12]. The lack of branches in the individual crystals coupled to small fractions of crystallinity were important microstructural features of our specimens to ensure that the stress fields did not overlap.

4.3. Physical properties

Fig. 2 shows the thermal expansion data for the glass sample and for fully crystallized samples obtained by a dilatometer (STA 409 Netzsch). To calculate their linear thermal expansion coefficients (α), the curves presented in Fig. 2 were fit by a linear function (Microcal Origin software, the correlation coefficients were $r = 0.998$ and $r = 0.999$ for the glass and fully crystallized samples, respectively) in a temperature range between 200°C and 400°C. The following are the *average* linear thermal expansion coefficients: $\alpha_g = 12.8 \times 10^{-6}$°C^{-1} for the glass and $\langle\alpha_c\rangle = 10.8 \times 10^{-6}$°C^{-1} for the fully crystallized sample. Typical errors are about $\pm 0.5 \times 10^{-6}$°C^{-1}. The αs are similar to those found by Freiman and Hench [13] in the same temperature range (12.5×10^{-6}°C^{-1} and 10.0×10^{-6}°C^{-1} for the glass and fully crystallized samples, respectively).

As α_g is larger than $\langle\alpha_c\rangle$, at first sight these results indicate that, if the embedded crystals are isotropic, they should be under *compression*. However, our experimental X-ray results indicated that, for some crystallographic planes, the embedded crystals were under *tension*. Thus we

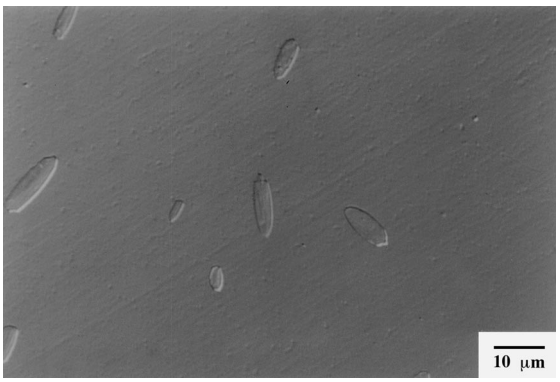

Fig. 1. RLM micrograph of the specimen heat-treated for 100 h at 460°C.

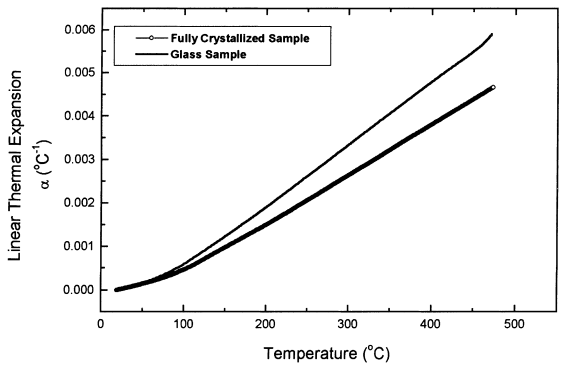

Fig. 2. Thermal expansion data for the glass and totally crystallized samples.

measured the linear thermal expansion coefficient for each (*hkl*) plane (α_{hkl}) through a hot stage X-ray diffraction camera. The measurements were made with a fully crystallized, stress-free, powdered specimen using an X-ray diffractometer (D-5000 Siemens). Both room and high (≈400°C) temperature experiments were made using a platinum-substrate heater attachment. The substrate was used as an internal standard. The diffraction peaks were recorded under the following conditions: Cu-Kα radiation, X-ray tube operated at 40 mA and 40 kV and a scintillation counter as detector. The diffraction peaks were collected at 25°C, 250°C and 400°C over the range of 20.0–75.0 (2θ) using a 0.01° step interval and a step time sufficient to give a signal to noise ratio. At each temperature, the substrate/sample assembly was heated for 10–20 min before measurement to ensure thermal equilibrium.

The linear thermal expansion coefficient, α_{hkl}, for each crystallographic plane was obtained by fitting linear functions to each d_{hkl} versus temperature curve (Microcal Origin software, r varied from 0.942 to 0.999). The results presented in Table 1 show that α_{hkl} is dependent on the (*hkl*) plane. For some crystallographic planes, the thermal expansion coefficient of the crystalline phase is larger than that of the glass matrix, while for other planes the inverse is observed. To compare these results with dilatometric data, we calculated the unit-cell volume change and then determined the volume expansion. According to Libeau, the $Li_2Si_2O_5$ phase has a monoclinic structure with an important orthorhombic pseudo-symmetry [14] i.e., $\beta \sim 90°$. Hence, to calculate the unit-cell volume, we used the following equations [15]:

$$\frac{1}{d^2} = \left(\frac{h^2}{a^2} + \frac{k^2}{b^2} + \frac{l^2}{c^2}\right), \tag{4}$$

$$V = abc, \tag{5}$$

where d is the interplanar spacing related to the (*hkl*) plane, a, b and c are the axial lengths and V the unit-cell volume.

The unit-cell parameters and the respective unit-cell volume at each temperature (25°C, 200°C and 400°C) were calculated using the following (*hkl*) planes: (0 1 0 0), (3 3 0) and (3 3 2). We have chosen crystallographic planes situated at larger angles because their angular position can be measured with better resolution. Using the interplanar spacings presented in Table 1 and Eqs. (4) and (5), we found the following unit-cell volumes: $V = 406.2$ Å^3 at 25°C, $V = 408.3$ Å^3 at 200°C, and $V = 410.8$ Å^3 at 400°C. The obtained data (volume cell versus temperature) was processed for linear curve-fitting (Microcal Origin software, $r = 0.999$). We found a volumetric coefficient of thermal expansion, $\alpha_V = (30.1 \pm 1.5) \times 10^{-6}$°C^{-1}. As α_V is approximately $3\alpha_{uc}$ (linear coefficient of thermal expansion), we found that α_{uc} is approximately equal to $(10.1 \pm 0.5) \times 10^{-6}$°C^{-1}. This α_{uc} is comparable to the average dilatometric $\langle\alpha_c\rangle$ found for the fully crystallized sample [$(10.8 \pm 0.5) \times 10^{-6}$°C^{-1}]. This result confirms the accuracy of our technique.

The moduli of elasticity (E) of the glass and of fully crystallized glass-ceramic were obtained using an ultrasonic technique (Quartz Resonant Oscillator mode). Bar shaped specimens ($12 \times 1 \times 1$ mm) of SiO_2 glass (used as a standard), Li_2O–$2SiO_2$ glass and fully crystallized Li_2O–$2SiO_2$ glass-ceramic were measured at room temperature. For the SiO_2 glass sample, we found $E = 71$ GPa, which is comparable to E found in the literature, 73 GPa [16].

For the lithium disilicate samples, we found an average E equal to 75 GPa for the glass and 122

Table 1
Thermal expansion coefficient obtained for each crystallographic (*hkl*) plane using a fully crystallized powder sample

(*hkl*)	2θ	α_{hkl} ($\times 10^{-6}$ °C^{-1})	$\Delta\alpha = (\alpha_{hkl} - \alpha_g) \times 10^{-6}$°C^{-1}
1 0 0	16.41	20.0	7.2
1 3 0	23.77	9.5	−3.3
0 4 0	24.39	5.3	−7.5
1 1 1	24.82	11	−1.8
2 0 0	30.69	17	4.2
0 0 2	37.57	8.3	−4.5
2 2 1	38.19	12.7	−0.1
3 3 0	50.60	16.0	3.2
1 1 −3	60.56	13.3	0.5
2 8 −1	63.14	13.6	0.8
0 10 0	63.68	6.8	−6.0
3 3 2	64.54	13.9	1.1
3 7 0	65.66	14.1	1.3

GPa for the glass-ceramic. According to the literature, the Young modulus of Li_2O–$2SiO_2$ glass varies from 72 to 82 GPa [16,17]. Young's modulus data for the Li_2O–$2SiO_2$ glass-ceramic are scarce. Freiman and Hench [13] reported that the Young modulus for a 90% crystallized Li_2O–$2SiO_2$ glass-ceramic is 127 GPa.

The Poisson ratios of the glass and fully crystallized glass-ceramic were taken from the literature [17,18]. The glass has a Poisson ratio, v between 0.22 and 0.23, whereas the fully crystallized (polycrystalline) material has an *average* Poisson ratio of 0.19. Since we did not find elastic properties data for single crystal $Li_2Si_2O_5$, these average E and v were used in our calculations to estimate the magnitude of both theoretical and experimental residual stresses.

4.4. Residual stress measurements

The XRD for measuring strains and stresses in crystalline solids is well established [19,20]. The method relies on using the crystal lattice as an absolute strain gauge [20]. XRD is based on Bragg's Law, which relates the interplanar spacing of atomic planes, d, to the angle peak position, θ, of a diffracted beam of monochromatic X-ray [15]. The residual strain determined by XRD is based on the displacement of the peaks in the XRD pattern, i.e., on the relative change in the interplanar distance of the crystalline phase under study when subjected to mechanical stresses. The relative deformation can be assessed from the displacement of the diffracted peaks as follows [20]:

$$\varepsilon_{hkl} = -0.5\Delta(2\theta)\cot(\theta) = \Delta d_{hkl}/d_{hkl}, \qquad (6)$$

where ε_{hkl} is the relative deformation of the crystal lattice normal to the (hkl) plane, $\Delta(2\theta)$ the displacement of the diffraction peak caused by the strain in the crystal, 2θ the Bragg angle and d_{hkl} the interplanar distance related to the (hkl) reflecting plane. The experimental residual stress can be determined by Hooke's Law:

$$\sigma_{\exp.} = \varepsilon_{hkl}E_{hkl}, \qquad (7)$$

where E_{hkl} is the direction dependent elastic modulus of the crystal.

X-ray diffraction measurements were carried out at the Synchrotron Light National Laboratory (LNLS-Campinas, Brazil) at 1.35 GeV, with a current between 70 and 120 mA. The experiments were made at room temperature and the X-ray beam was monochromatized using a Si(1 1 1) double-crystal. A scintillation counter was used as detector. Data for the glass-ceramic monolithic samples and for the fully crystallized sample were collected over a 2θ range of 45.0–75.0°, using a 0.02° (2θ) step interval. Due to the volume fraction of crystals in the partially crystallized glass-ceramics (~10%), each XRD spectra was collected during 4 h. It was possible to measure the position of six different interplanar spacings with a reasonable signal to noise ratio (5) in this 2θ range.

As an example, we present X-ray curves for the fully crystallized sample and for a partially crystallized glass-ceramic (100 h treatment) in Figs. 3 and 4. The X-ray diffraction spectrum of the sample heated for 100 h shows that, due to the quality of the crystals, some peaks are detected. Both spectra present only the $Li_2Si_2O_5$ crystalline phase (JCPDS 17-447). The internal residual strain and stresses presented in Table 2 were calculated using Eqs. (6) and (7). The type of experimental residual stress show that the crystals embedded in the glass matrix are in tension for $\langle\alpha_c\rangle$ larger than α_g and in compression for $\langle\alpha_c\rangle$ smaller than α_g. Regarding the stress magnitude, the experimental

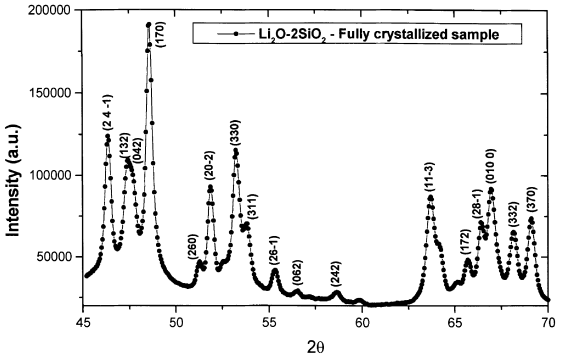

Fig. 3. X-ray curve for the fully crystallized sample (24 h at 450°C and 20 min at 600°C). The diffraction peaks in the figure are identified with their respective (hkl) plane.

Table 2
X-ray diffraction data, experimental and theoretical internal strain and stresses using Eqs. (6) and (7)

Sample	Sample form	(*hkl*)	2θ	d (Å)	ε ($\times 10^{-3}$)	$\sigma_{exp.}$ (MPa)	$\sigma_{Theo.}$ (MPa)
Fully crystallized [a]	Powder	3 3 0	53.27	1.7935	–	–	–
Fully crystallized	Powder	1 1 −3	63.71	1.5234	–	–	–
Fully crystallized	Powder	2 8 −1	66.46	1.4672	–	–	–
Fully crystallized	Powder	0 10 0	66.96	1.4576	–	–	–
Fully crystallized	Powder	3 3 2	68.14	1.4352	–	–	–
Fully crystallized	Powder	3 7 0	69.08	1.4181	–	–	–
86 h 460°C	Plate	3 3 0	53.20	1.7957	1.22	149	102
86 h 460°C	Plate	1 1 −3	63.66	1.5245	0.72	88	16
86 h 460°C	Plate	2 8 −1	66.40	1.4686	0.81	98	25
86 h 460°C	Plate	0 10 0	66.99	1.4569	−0.48	−58	−192
86 h 460°C	Plate	3 3 2	68.06	1.4366	0.97	118	35
86 h 460°C	Plate	3 7 0	69.04	1.4188	0.49	60	42
100 h 460°C	Plate	3 3 0	53.22	1.7951	0.89	108	102
100 h 460°C	Plate	1 1 −3	63.63	1.5252	1.18	143	16
100 h 460°C	Plate	2 8 −1	66.38	1.4686	0.95	116	25
100 h 460°C	Plate	0 10 0	67.03	1.4562	−0.96	−117	−192
100 h 460°C	Plate	3 3 2	68.08	1.4364	0.83	101	35
100 h 460°C	Plate	3 7 0	69.02	1.4192	0.77	94	42

[a] Fully crystallized = 24 h at 450°C, 10 min at 600°C.

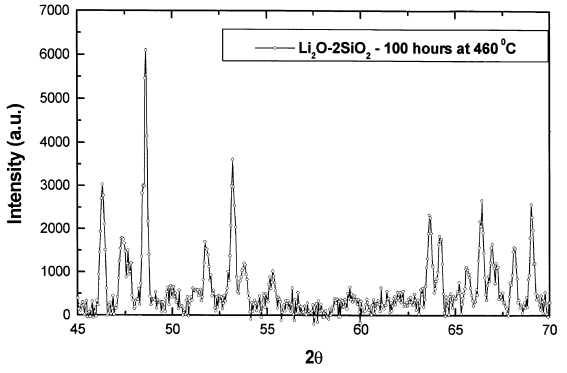

Fig. 4. X-ray curve for a partially crystallized glass-ceramic (100 h at 460°C).

σs vary from −58/−117 MPa (compressive) to 60/149 MPa (tensile).

5. Residual stress calculations

The stresses at the particle/matrix interface were calculated using Eq. (1) and the Selsing formula (3). The following data were used: $\Delta\alpha = (\alpha_{hkl} - \alpha_g)$ *for each crystallographic plane* (presented in Table 1); $\Delta T = 425$°C (we consider a temperature range in which the matrix plasticity is negligible, from T_g to room temperature); $\nu_m = 0.23$; $\nu_p = 0.19$, $E_m = 7.5 \times 10^4$ MPa and $E_p = 12.2 \times 10^4$ MPa. Due to the lack of single crystal data for the elastic constants, *averages* ν_p and E_p (obtained for polycrystalline samples) were used. Substituting these averages into Eq. (3), we found that the *calculated* σs vary from −192 MPa (compressive) to 16/102 MPa (tensile). As the experimental errors in these measurements are about 20%, the differences between the theoretical and experimental stress magnitudes are within the error limits. The results for each crystal plane are presented in Table 2.

An attempt was made to estimate the magnitude of residual stresses using micro-Raman spectroscopy technique [21]. The residual stresses can be obtained by measuring the shifts of the Raman lines of the polycrystalline samples. Raman spectra were obtained with a Raman microprobe consisting of a microscope (Olympus BH-2) equipped with a holographic beam splitter and a super nutch filter. A nominal 10 mW HeNe laser was used as the excitation source. Pressure was generated in a diamond anvil cell (DAC) and measured with the ruby fluorescence technique

[22]. Experiments with the powder sample were performed with silicon oil. A more detailed description of Raman experiments can be found in Ref. [23]. A calibration curve was constructed with the fully crystallized Li_2O–$2SiO_2$ powder, which indicated that the detection limit of the equipment used was about 150 MPa. As no detectable shift was observed in the micro-Raman lines of our monolithic glass-ceramics when compared to the spectrum of a fully crystallized (stress free) powder, we conclude that the magnitude of residual stress in the glass-ceramics was <150 MPa.

Taking into account the fact that the thermal expansion coefficient of the crystal is anisotropic, our experimental results and theoretical calculations concerning the *type* of residual stress agree. As can be noted in Table 2, however, there are differences between the theoretical and experimental stress *magnitudes* for each crystallographic plane. On the other hand, these differences are within the limits of experimental error. Due of the lack of data for single crystals, we assumed in our calculations that the Young modulus and the Poisson ratio of the crystalline phase are isotropic. If we take into account the uncertainty which results from this approximation, the overall magnitude of the theoretical and experimental residual stress are consistent with the Raman spectroscopy estimate.

Mathematical solutions for anisotropic stresses adjacent to odd-shaped crystals in commercial glass-ceramics containing a volume fraction $\geqslant 15\%$ of crystals are complex and should be solved using finite element computer simulations.

6. Conclusions

It is necessary to take into account the anisotropy of the thermal expansion coefficient and elastic constants of silicate crystals to make a proper evaluation of residual stresses in glass-ceramics. For the lithium silicate glass-ceramic studied here, these stresses were compressive or tensile, depending on the crystallographic direction, and varied from about -120 MPa to +150 MPa. The theoretical and experimental stresses agreed within experimental error, therefore, the Selsing model can give a reasonable estimate of residual stresses even for real, anisotropic, materials.

These stresses have an effect on the mechanical properties of glass-ceramics and should be taken into account by researchers interested in their mechanical properties.

Acknowledgements

We are indebted to Professors Richard Bradt, Luis N. Oliveira and Walter Libardi for stimulating discussions. We also thank Professor João A.H. da Jornada for the Raman spectroscopy measurements. The financial help of FAPESP and PRONEX are fully appreciated. This research was partially performed at LNLS National Synchrotron Light Laboratory, Brazil.

References

[1] G. Partridge, Glass Technol. 35 (1994) 116.
[2] D.W. Jones, Key Eng. Mat. 122 (1996) 345.
[3] Glass Sci. Technol., cover page 68 (1995).
[4] V.R. Mastelaro, E.D. Zanotto, J. Non-Cryst. Solids 194 (1996) 297.
[5] J. Selsing, J. Am. Ceram. Soc. 44 (1961) 419.
[6] R.M. Fulrath, J. Am. Ceram. Soc. 42 (1959) 423.
[7] L.A. Zevin, E.A. Levy, Z.G. Bessmertnaya, Neorg. Mater. 13 (1977) 1880.
[8] R.W. Davidge, T.J. Green, J. Mater. Sci. 3 (1968) 629.
[9] M.P. Borom, A.M. Turkalo, R.H. Doremus, J. Am. Ceram. Soc. 58 (1975) 385.
[10] N. Miyata, K. Tanigawa, H. Jinno, Fracture Mechanics of Ceramics, vol. 5, Plenum, New York, 1983, p. 609.
[11] E.D. Zanotto, M.L. Gomes Leite, J. Non-Cryst. Solids 202 (1996) 145.
[12] P.F. James, Y. Iqbal, U.S. Jais, S. Jordery, W.E. Lee, J. Non-Cryst. Solids 219 (1997) 17.
[13] S.W. Freiman, L.L. Hench, J. Am. Ceram. Soc. 55 (1972) 86.
[14] F. Libeau, Acta Crystallogr. 14 (1961) 389.
[15] B.D. Cullity, Elements of X-Ray Diffraction, 2nd ed., Addison–Wesley, Reading, MA, 1978, p. 292.
[16] N.P. Bansal, R.H. Doremus (Eds.), Handbook of Glass Properties, Academic Press, New York, 1986.
[17] INTERGLAD, International Glass Database, New Glass Forum, Tokyo, Japan, 1991.
[18] J.Y. Thompson, PhD thesis, University of Florida, 1995.

[19] J.C. Noyau, J.B. Cohen, Residual Stress: Measurements by X-ray Diffraction and Interpretation, Springer, New York, 1987, p. 117.
[20] A. Abuhasan, C. Balasingh, P. Predecki, J. Am. Ceram. Soc. 73 (1990) 2474.
[21] G. Lucazeau, L. Abello, Analysis 23 (1995) 301.
[22] G.J. Piermarini, S. Block, Rev. Sci. Instrum. 46 (1975) 973.
[23] C.A. Perottoni, J.A.H. da Jornada, Science 886 (1998) 886.